ARTICLE IN PRESS
MARCHE-02992; No of Pages 15
Marine Chemistry xxx (2013) xxx–xxx
Contents lists available at SciVerse ScienceDirect
Marine Chemistry
journal homepage: www.elsevier.com/locate/marchem

Submarine groundwater discharge in a river-dominated Florida estuary

Matthew A. Charette [a,*], Paul B. Henderson [a], Crystaline F. Breier [a], Qian Liu [b]

[a] Department of Marine Chemistry and Geochemistry, Woods Hole Oceanographic Institution, Woods Hole, MA 02543, USA
[b] State Key Lab of Marine Environmental Science, Xiamen University, Xiamen 361005, China

ARTICLE INFO

Available online xxxx

Keywords:
Radium isotopes
Groundwater
Estuarine dynamics
Nitrogen
Nutrients

ABSTRACT

Eutrophication in the coastal zone has largely been driven by changing land use practices that lead to nutrient-enhanced runoff. While in most studies the overland component of this nutrient vector has been well documented, the role of groundwater in coastal nutrient mass balances is often poorly constrained. Here, we used radium isotopes to quantify SGD and associated nutrient fluxes to the Caloosahatchee River estuary (Florida, USA) during the wet and dry seasons of 2009–2010. Like many estuaries worldwide, the nutrient balance and ecology of the Caloosahatchee has been negatively impacted by excessive nutrient-laden runoff from fertilizer use and other anthropogenic sources. A four endmember mixing model was used to quantify the magnitude of SGD and the relative importance of terrestrial and marine groundwater sources. Terrestrial groundwater comprised 44% of the total SGD in April 2009, but 98–100% of the total groundwater flux during all other time periods. SGD rates were highly seasonal ranging from a low of 8.5×10^4 m^3 d^{-1} in April 2010 to a high of 1.3×10^6 m^3 d^{-1} in October 2010 (average $= 4.8 \pm 5.5 \times 10^5$ m^3 d^{-1}). For the four time periods, these fluxes ranged from 2 to 140% (average = 43%) of the river discharge through Franklin Lock, a water control structure at the head of the estuary and the only previously quantified source of nutrients to the system. The groundwater total dissolved nitrogen (TDN) flux to the estuary averaged 450 ± 490 kg d^{-1} for the four time periods, while dissolved inorganic nitrogen (DIN) and soluble reactive phosphorous (SRP) averaged 241 ± 267 kg d^{-1} and 93 ± 111 kg d^{-1}, respectively. On average, the surface water freshwater fluxes for TDN exceeded the SGD fluxes by a factor of 6. However, the SGD fluxes of DIN and SRP, highly bioavailable forms of N and P, were only 3 and 1.5 times lower than the river flux, respectively. The major form of nitrogen carried by groundwater to the estuary was ammonium; this highly labile form of nitrogen is likely rapidly consumed within the estuary by primary producers (both macro- and microalgae). Our results suggest that during extended dry periods when water releases from Franklin Lock are at a minimum, SGD will remain a substantial source of nutrients to the system.

1. Introduction

Constructing nutrient budgets for coastal waters requires a comprehensive understanding of the local water cycle (Slomp and Van Cappellen, 2004). One aspect of the water cycle that has received growing attention is submarine groundwater discharge (SGD), which is known to convey nutrients to coastal waters (Charette et al., 2001; Paytan et al., 2006; Boehm et al., 2006; Weinstein et al., 2011). Historically, a lack of widely available tools and techniques for quantifying the water flux has been an obstacle to inclusion of SGD in coastal nutrient mass balances. The past decade, however, saw a concerted effort to develop a series of new techniques based on chemical tracers and validate them against well established traditional hydrogeologic approaches (Burnett et al., 2006).

One newly developed methodological approach is based on the use of radium isotopes, which takes advantage of radium's natural enrichment in groundwater relative to other sources of water to the coastal zone such as rivers and precipitation. Radium has been shown to be a useful indicator of SGD, which has been defined as the advective flow of groundwater (irrespective of its salinity) into the coastal zone (Moore, 1996; Rama and Moore, 1996; Charette et al., 2001). Furthermore, radium has four isotopes with half-lives ranging from 4 days to 1600 years (^{224}Ra, $t_{1/2} = 3.66$ days; ^{223}Ra, $t_{1/2} = 11.4$ days; ^{228}Ra, $t_{1/2} = 5.75$ years; ^{226}Ra, $t_{1/2} = 1600$ years). As such, it may be used to deconvolve various groundwater sources (e.g. shallow vs. confined aquifers; Charette and Buesseler, 2004) or estimate coastal mixing rates (Moore, 2000) necessary for calculating Ra fluxes to quantify SGD. If the radium excesses in estuarine and coastal surface waters can be attributed to SGD, then simultaneous measurements of nutrient concentration in the water column and groundwater can be used to derive the SGD associated nutrient flux to the coastal zone (Krest et al., 2000; Charette et al., 2001; Paytan et al., 2006).

There is growing evidence that SGD may be an important nutrient source in Florida coastal waters. Before SGD was widely recognized

* Corresponding author. Tel.: +1 508 289 3205; fax: +1 508 457 2193.
E-mail address: mcharette@whoi.edu (M.A. Charette).

0304-4203/$ – see front matter © 2013 Elsevier B.V. All rights reserved.
http://dx.doi.org/10.1016/j.marchem.2013.04.001

for its potential to impact coastal ocean geochemical budgets, Miller et al. (1990) concluded that groundwater was a major source of ^{226}Ra to the Charlotte Harbor estuary. More recently, Swarzenski et al. (2007) noted that SGD accounted for over half of the total nitrogen inputs to Tampa Bay. Furthermore, Hu et al. (2006) suggested that there is a link between SGD driven by large scale precipitation associated with hurricane passage and HABs in this area. Indeed, radon and radium-derived SGD associated nutrient fluxes to the west Florida shelf have been shown to be a necessary component of the nutrient standing stock required for HAB maintenance and growth (Smith and Swarzenski, 2012).

Here, we use radium isotopes to estimate SGD and associated nutrient fluxes to the Caloosahatchee River estuary (Florida, USA) during the wet and dry seasons of 2009–2010. Like many estuaries worldwide, the nutrient balance and ecology of the Caloosahatchee has been negatively impacted by excessive nutrient-laden runoff from fertilizer use and other anthropogenic activities (Brand and Compton, 2007; Lapointe and Bedford, 2007). Brand and Compton (2007) noted the potential effect that canal construction, which connected Lake Okeechobee to the Caloosahatchee River watershed, had on the nutrient flux to that system and the associated abundance of the toxic dinoflagellate *Karenia brevis* along the west Florida shelf. Using stable nitrogen isotopes, Lapointe and Bedford (2007) linked the presence of the nuisance drift algae to sewage nutrient sources associated with freshwater releases to the Caloosahatchee River through the Franklin Lock. While they suggested that groundwater-derived nutrient inputs to the Caloosahatchee River might have played a role in the blooms, they did not have SGD estimates to quantify its relative importance.

2. Methods

2.1. Study area

The Caloosahatchee River estuary is the conduit for one of the four largest river discharges along the west coast of Florida. It is bounded by San Carlos Bay and the Gulf of Mexico to the west and the Franklin Lock/Dam (S-79) to the east, a length of approximately 50 km (Fig. 1). Within the estuary, the tidal range is on the order of 40 cm. The lock is maintained by the Army Corps of Engineers, and water releases are not only used to maintain certain water levels on the inland side of the dam but are also used to maintain a natural salinity balance within the estuary (SFWMD, 2012). Annual discharge at S-79 averaged 5.7×10^6 m^3 d^{-1} during 1995–2008; wet season flow was approximately 2 times higher than in the dry season (3.7×10^6 vs. 2.0×10^6 m^3 d^{-1}; SFWMD, 2012). This same pattern was generally observed during the 2-year time frame of this study (Fig. 2a).

Rainfall over the watershed averaged 30.7 cm in the dry season (Nov.–Apr.) and 95.5 cm in the wet season (May–Oct.) for the period 1996–2008 (SFWMD, 2012). The watershed surrounding the estuary is densely populated (cities of Ft. Myers and Cape Coral), while land use east of Franklin Lock is mostly agricultural. The surficial unconfined aquifer system (30–40 m thick) consists of three units of a quartz sand unit, a mixed sand/shell unit, and a unit with sandy limestone/quartz sand/clayey sands (Reich, 2009). Groundwater elevations are typically correlated with rainfall patterns, with peak groundwater inventories occurring in mid-summer (Fig. 2b). The lower Tamiami aquifer is also considered to be a part of the surficial aquifer system; it is separated from the upper surficial aquifer by a semiconfining unit that retards but does not entirely prevent exchange (Krulikas and Geise, 1995). The first and second confining units are the Hawthorne aquifer and the upper Floridan aquifer, respectively. The lower Hawthorne and upper Floridan are artesian in monitoring wells at the coast, but are not believed to exchange with the surficial aquifer system and do not outcrop within the estuary or its watershed (Cunningham et al., 2001). In contrast, Krulikas and Geise (1995) mapped the groundwater potentials for a number of surficial groundwater monitoring wells bordering the Caloosahatchee; hydraulic gradients were as high as 0.001 along the south-central and northeastern estuarine shorelines, decreasing with the land topography to lower values near the estuary mouth.

This study was carried out during four time periods: April 2009 and 2010 and October 2009 and 2010. The April and October time points were chosen in order to capture conditions at the ends of the dry and wet seasons, respectively. However, rainfall leading up to the April 2009 sampling was about half the long term dry season average (15 cm), while the 2010 dry season was unusually wet (54 cm). This abbreviated dry season is reflected in the relatively early and rapid rise in surficial groundwater inventories in late January through early February 2010 (Fig. 2b). The two October sampling periods were characterized by relatively normal rainfall conditions during the wet season (within ~20% of the long term average); peak groundwater levels during the preceding summers were largely the same (Fig. 2b). Discharges at Franklin Lock were generally reflective of the precipitation patterns over the watershed, though water fluxes in both years were approximately 15% below the long term average (4.8 vs. 5.7×10^6 m^3 d^{-1}), a result of drought conditions in the years preceding our study (SFWMD, 2012) (Fig. 2a).

During each time period, samples were collected from the estuary water column and groundwater. The estuary stations spanned from

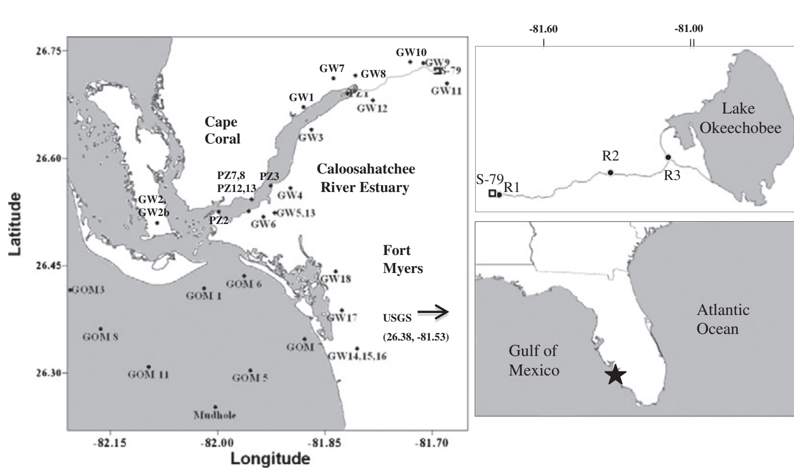

Fig. 1. Map of the study area including station locations for the samples listed in Tables 1–4. Not shown are the estuary stations (E1–E44), which were chosen based on the estuarine salinity distribution at the time of sampling rather than fixed locations.

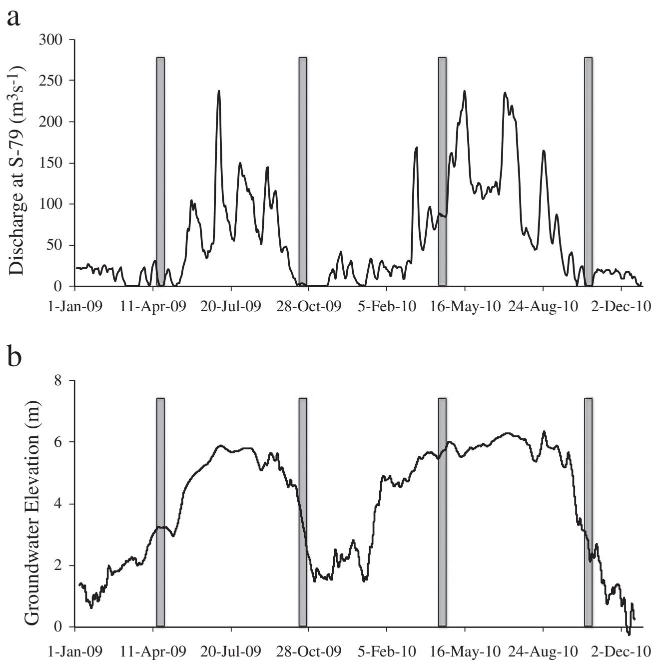

Fig. 2. (a) One-week running average of daily mean discharge at the S-79 dam (Franklin Lock) for 2009–2010 (South Florida Water Management District DBHYDRO website: http://www.sfwmd.gov/, DB Key P1023). (b) One-week running average of groundwater elevation for 2009–2010 (elevation above NGDV 1929; USGS Well 262248081314101 C-1244). See Fig. 1 for the location of the USGS monitoring well. Gray bars indicate the 3-day sampling window for each of the four study periods.

the Gulf of Mexico through to the freshwater side of the Franklin Lock (Fig. 1). In some seasons, samples were collected as far east as the outlet from Lake Okeechobee. Groundwater samples were collected from the estuary margins, mainly from wells maintained by Lee County Natural Resources, but also from piezometers installed by our group. Most monitoring wells were located within the unconfined surficial aquifer, though two were cased within the upper middle and lower middle Hawthorne confining unit. The latter well was artesian (~3–4 m above sea level) each time it was sampled in 2009.

2.2. Field and laboratory protocols

For radium isotopic analysis within the estuary, 20–100 L of water was filtered into a plastic container, which was then slowly pumped or gravity fed (<1 L min^{-1}) through MnO_2 coated acrylic fiber to extract the Ra (Moore and Reid, 1973). Samples for nutrients were collected into 20 mL, acid cleaned scintillation vials using a capsule filter (Pall Acropak, 0.22 μm). Basic water properties including salinity, pH, dissolved oxygen, and redox potential were recorded with the YSI sonde.

Groundwater samples were collected from various locations along the estuary edge and from various depths within the surficial aquifer (Fig. 1). Estuarine groundwater samples were collected with Push Point samplers (MHE Products, Inc.). Briefly, the stainless steel piezometer was driven to the depth of interest. Samples were pumped through plastic tubing using a peristaltic pump. When sampling from monitoring wells, we used a plastic submersible well pump (Proactive Monsoon with Power Booster 2). In either case, water was pumped 3× the well boring volume prior to sampling; a YSI sonde was placed in line such that water chemistry could be monitored during the flushing of the piezometer or monitoring well. For Ra analysis, groundwater was pumped directly through the Mn fiber (10–20 L) and the filtrate was collected to determine the sample volume. Samples for nutrients were collected as above with the exception of a second sample, which was stored acidified for total dissolved phosphate analysis.

To quantify the potential contribution of radium-desorption from suspended sediments to the radium mass balance in the estuary, we pumped ~500 L of river water from the freshwater side of the Franklin Lock through a 1 μm Hytrex polypropylene cartridge filter. The filter was dried, ashed, and analyzed via gamma spectrometry according to the methods described below for MnO_2 fiber.

Back in the laboratory, the MnO_2-fiber was rinsed with DI water and partially dried. Activities of ^{223}Ra ($t_{1/2} = 11.4$ days) and ^{224}Ra ($t_{1/2} = 3.66$ days) were measured on a delayed coincidence counter as described by Moore and Arnold (1996). The fiber was then ashed in a muffle furnace (820 °C for 16 h), ground, and homogenized, then packed in a counting vial and sealed with epoxy to prevent ^{222}Rn loss (Charette et al., 2001). Once ^{222}Rn had reached secular equilibrium with its parent, activities of ^{226}Ra ($t_{1/2} = 1600$ years) and ^{228}Ra ($t_{1/2} = 5.75$ years) were determined by γ-counting in a well detector (Canberra, model GCW4023) by the ingrowth of ^{214}Pb (352 keV) and ^{228}Ac (911 keV). Calibration of the well detector was achieved by counting four ashed MnO_2 fiber standards within the same activity range and geometry of the samples. Nutrient analyses (nitrate, phosphate, ammonium, silicate) were performed using standard methods on a Lachat QuickChem 8000 Flow Injection Analyzer. Total dissolved nitrogen (TDN) was determined using persulfate oxidation followed by nitrate analysis as above.

3. Results

3.1. Groundwater radium

Groundwater ^{226}Ra activities were among the highest we have observed in nearly 15 years studying submarine groundwater discharge (Tables 1–4). The key influence appears to be local deposits of phosphorite, a naturally occurring phosphate-bearing mineral that also contains appreciable quantities of uranium and its decay products (Miller et al., 1990; Cowart and Burnett, 1994). This is supported not only by high ^{226}Ra, but also by the relatively low average groundwater ^{228}Ra/^{226}Ra (0.20), which deviates significantly from the crustal average of ~1 due to U enrichment and Th depletion in such mineral deposits (Crotwell and Moore, 2003). The average ^{226}Ra for April-09, Oct-09, April-10, and Oct-10 was 795, 582, 878, and 920 dpm 100 L^{-1}, respectively (not shown). Hence, there was no discernable seasonable variability in the groundwater ^{226}Ra.

We also examined the distribution of Ra isotopes relative to salinity and the sampled aquifer formation (Fig. 3). Given radium's lower partition coefficient under high ionic strength (Gonneea et al., 2008), it is notable that radium was enriched despite the low average salinity of the monitoring wells (3.0, 2.9, 4.8, and 5.6 for April-09, Oct-09, April-10, and Oct-10, respectively). However, there was a salinity dependence for our groundwater Ra dataset: the average ^{226}Ra for brackish or saline monitoring wells and piezometers (salinity > 3 with an average salinity of ~20) was 3180 dpm 100 L^{-1}, while our low salinity average was 730 dpm 100 L^{-1} (Fig. 3). Furthermore, the brackish groundwater was more enriched in ^{228}Ra than the low salinity groundwater with average ^{228}Ra/^{226}Ra ratios of 0.15 and 0.07, respectively. Miller et al. (1990) hypothesized that the elevated groundwater ^{226}Ra activities they observed beneath Charlotte Harbor were because sea level rise had increased groundwater salinity and thus released ^{226}Ra from aquifer materials through ion exchange.

We also examined the Ra isotope distribution between the different aquifer formations (Fig. 3). Of the low salinity (hereafter termed "terrestrial") groundwater sources, the lower Hawthorne aquifer had the highest average ^{226}Ra (2180 dpm 100 L^{-1}) and lowest ^{228}Ra/^{226}Ra ratio (0.05). The upper Hawthorne and deep surficial groundwater had similar ^{226}Ra activities (315 and 299 dpm 100 L^{-1}, respectively) but very different ^{228}Ra/^{226}Ra ratios (0.09 vs. 0.32). The shallow surficial aquifer terrestrial groundwater samples averaged 722 dpm 100 L^{-1} in ^{226}Ra with a ^{228}Ra/^{226}Ra ratio of 0.17.

Please cite this article as: Charette, M.A., et al., Submarine groundwater discharge in a river-dominated Florida estuary, Mar. Chem. (2013), http://dx.doi.org/10.1016/j.marchem.2013.04.001

Table 1
April 2009 nutrient concentrations and radium activities from the Caloosahatchee River Estuary groundwater study.

Station ID	WHOI ID	Sample type	Latitude (°N)	Longitude (°W)	Salinity	SiO_4^-	PO_4^{3-}	$NO_3^- + NO_2^-$	NH_4^+	TDN	^{224}Ra	^{223}Ra	^{226}Ra	^{228}Ra	Water age (days)	Monitoring well depth (m)*	Aquifer formation
						(μmol L^{-1})					(dpm 100 L^{-1})						
G1	GOM01	GoM surface	26.4182	−82.0190	36.36	4.5	<0.05	< 0.05	3.7		5.5	4.0	36.8	19.0	22.6		
G3	GOM03	GoM surface	26.4160	−82.2061	36.28	2.6	<0.05	0.08	3.8	9.3	3.3	1.1	22.1	9.4	17.8		
G5	GOM05	GoM surface	26.3040	−81.9541	36.61	7.8	<0.05	<0.05	4.2		6.7	6.7	61.7	36.9	39.8		
G6	GOM06	GoM surface	26.4353	−81.9631		3.0	<0.05	0.16	5.2	29.1	24.4	13.2	74.1	42.4	8.8		
G7	GOM07	GoM surface	26.3470	−81.8780		4.0	<0.05	<0.05	4.2	20.6	10.5	11.2	68.4	36.1	22.5		
G8	GOM08	GoM surface	26.3612	−82.1631	36.34	10.7	0.10	0.51	5.9	10.6	2.0	1.4	18.8	8.0	27.2		
G11	GOM11	GoM surface	26.3087	−82.0963	36.26	5.6	0.40	<0.05	5.5		5.6	4.6	47.2	21.2	25.6		
Mudhole	GOM_MUDHOLE	GoM surface	26.2523	−82.0027	36.45	5.1	0.00	0.54	3.0		4.2	4.5	55.7	29.2	51.4		
E1	CAL1	Cal. estuary	26.6781	−81.8385	9.54	23.2	1.67	1.07	1.3		19.5	10.7	290.4	36.2	9.8		
E2	CAL2	Cal. estuary	26.6973	−81.7991	5.46	15.5	1.11	3.69	3.8	34.0	13.1	6.7	280.7	33.9	15.8		
E3	CAL3	Cal. estuary	26.7215	−81.7339	3.26	23.7	1.64	4.61	3.9	48.4	6.5	17.4	195.1	20.3	20.3		
E4	CAL4	Cal. estuary	26.7234	−81.7006	2.52	54.6	3.01	7.62	4.2	68.2	7.4	4.7	190.8	20.4	17.1		
E5	CAL5	Cal. estuary	26.4837	−82.0156	35.82	19.3	0.60	0.54	5.0		38.6	21.0	103.4	47.9	4.8		
E6	CAL6	Cal. estuary	26.5232	−82.0076	32.87	17.2	0.60	0.71	9.3	27.0	33.9	23.7	200.7	62.5	9.7		
E7	CAL7	Cal. estuary	26.5312	−81.9597	27.78	19.6	0.99	0.29	5.6		23.9	27.9	287.1	68.6	18.0		
E8	CAL8	Cal. estuary	26.5573	−81.9301	24.88	10.3	0.92	0.36	5.4	40.4	21.2	18.3	381.8	74.7	23.3		
E9	CAL9	Cal. estuary	26.6094	−81.8964	19.75	18.6	1.85	0.40	2.1		25.2	14.8	508.0	78.9	20.2		
E10	CAL10	Cal. estuary	26.6483	−81.8724	17.35	11.7	0.95	0.71	3.3		26.7	17.4	439.8	62.6	13.8		
R1	CAL11	Cal. river	26.7211	−81.6922	0.35	66.3	2.45	8.20	3.2	79.8	3.7	2.5	13.0	14.6	26.5		
R2	CAL12	Cal. river	26.7885	−81.3030	0.26	82.5	0.94	3.39	1.3	89.3	6.0	2.2	71.8	13.8	13.5		
R3	CAL13	Cal. river	26.8394	−81.0809	0.28	113.7	0.93	9.83	5.1	78.3	10.9	1.6	6.6	18.5	8.5		
GW1	FGCU_GW1	Monit. well	26.6711	−81.8799	0.26	144.6	5.10	0.78	24.0	81.7	14.0	8.6	49.0	8.7		5.9 (4.3)	Upper surficial
GW2	FGCU_GW2	Monit. well	26.5100	−82.0846		62.8	9.53	0.32	130.7	169.4	214.2	41.5	485.2	279.9		6.6 (4.9)	Upper surficial
GW2B	FGCU_GW2b	Monit. well	26.5100	−82.0846	42.00						709.7	143.4	2443.9	945.4		6.6 (4.9)	Upper surficial
GW3	FGCU_GW3	Monit. well	26.6397	−81.8689	0.40	60.2	2.15	0.58	10.4	29.7	38.3	12.4	428.1	32.2		8.2 (6.6)	Upper surficial
GW4	FGCU_GW4	Monit. well	26.5588	−81.8982	0.43	88.3	1.91	0.76	28.5	122.6	56.1	24.9	308.0	59.3		6.6 (4.9)	Upper surficial
GW5	FGCU_GW5	Monit. well	26.5238	−81.9202	1.53	154.1	1.74	0.65	76.5	92.0	58.3	48.5	735.0	87.6		5.9 (4.6)	Upper surficial
GW6	FGCU_GW6	Monit. well	26.5185	−81.9357	1.16	89.7	11.66	0.38	57.0	100.3	65.4	63.3	2160.8	90.4		5.9 (5.2)	Upper surficial
GW7	FGCU_GW7	Monit. well	26.7114	−81.8382	0.29	108.6	34.79	1.80	53.8	70.8	28.6	7.6	86.3	15.6		9.2 (7.9)	Upper surficial
GW8	FGCU_GW8	Monit. well	26.7158	−81.8072	0.65	204.6	20.34	0.82	16.8	28.2	32.2	21.7	154.1	9.9		5.9 (4.3)	Upper surficial
GW9	FGCU_GW9	Monit. well	26.7332	−81.7128	0.39	166.7	4.94	0.30	63.3	88.4	32.1	43.9	1527.7	43.4		6.5 (5.2)	Upper surficial
GW10	FGCU_GW10	Monit. well	26.7346	−81.7309	0.43	161.1	0.46	7.76	19.5	47.4	49.3	14.5	162.1	30.4		6.5 (5.2)	Upper surficial
GW11	FGCU_GW11	Monit. well	26.7046	−81.6797	0.23	167.9	0.55	0.76	24.2	40.1	23.3	29.5	492.6	21.8		8.9 (6.6)	Upper surficial
GW12	FGCU_GW12	Monit. well	26.6805	−81.7832	0.22	81.4	1.71	0.52	4.3	38.6	26.3	13.2	128.8	21.2		6.6 (4.9)	Upper surficial
GW13	FGCU_GW13	Monit. well	26.5238	−81.9202	0.37	229.5	0.48	0.55	15.5	40.4	11.8	9.3	255.5	24.3		101 (NA)	Upper mid. Hawthorne
GW14	FGCU_GW14	Monit. well	26.3339	−81.8046	3.64	239.5	0.30	0.10	26.9	36.1	93.6	272.3	3445.5	47.0		154 (NA)	Lower mid. Hawthorne
GW15	FGCU_GW15	Monit. well	26.3339	−81.8046	2.25	283.6	0.87	0.92	29.3	49.9	122.6	129.2	1214.3	79.5		5.9 (4.6)	Upper surficial
GW16	FGCU_GW16	Monit. well	26.3339	−81.8046	0.80	99.7	4.06	3.33	97.7	189.0	139.6	28.6	342.6	94.3		39 (NA)	Lower surficial
GW17	FGCU_GW17	Monit. well	26.3875	−81.8262	0.37	32.8	4.84	0.68	26.3	48.4	139.4	12.2	141.7	129.6		6.9 (4.9)	Upper surficial
GW18	FGCU_GW18	Monit. well	26.4419	−81.8346	0.25	62.5	0.37	0.94	29.9	45.7	52.9	28.9	234.9	20.3		6.6 (4.9)	Upper surficial

Table 2
October 2009 nutrient concentrations and radium activities from the Caloosahatchee River Estuary groundwater study.

Station ID	WHOI ID	Sample Type	Latitude (°N)	Longitude (°W)	Salinity	SiO_4^-	PO_4^{3-}	$NO_3^- + NO_2^-$	NH_4^+	TDN	^{224}Ra	^{223}Ra	^{226}Ra	^{228}Ra	Water age (days)	Monitoring well depth (m)*	Aquifer formation
						(μmol L^{-1})					(dpm 100 L^{-1})						
G1	GOM01A	GoM surface	26.4190	−82.0222	35.03	15.9	<0.05	0.1	0.8	18.2	8.1	5.8	63.6	24.7	19.6		
G3	GOM03A	GoM surface	26.4160	−82.2061	35.39	18.3	< 0.05	0.2	1.0	16.1	8.6	4.8	55.1	22.3	15.9		
G5	GOM05A	GoM surface	26.3038	−81.9540	35.89	6.6	<0.05	2.3	1.4	17.0	3.4	2.5	53.3	20.5	44.2		
G6	GOM06A	GoM surface	26.4397	−81.9623		26.0	0.1	0.7	2.0	21.6	17.2	9.9	74.5	29.0	8.4		
G7	GOM07A	GoM surface	26.3469	−81.8778	35.55	11.6	<0.05	0.5	0.4	22.2	6.7	4.8	71.7	28.2	29.2		
G8	GOM08A	GoM surface	26.3612	−82.1630	36.14	5.5	<0.05	0.3	0.6	27.3	3.1	2.3	61.6	21.2	50.2		
G11	GOM11A	GoM surface	26.3086	−82.0963	35.80	6.6	<0.05	0.6	1.7	12.8	20.5	2.0	52.0	19.1	2.3		
E11	CAL1A	Cal. estuary	26.6469	−81.8744	6.33	53.7	2.6	1.7	0.2	33.9	10.0	8.9	242.1	27.7	17.2		
E12	CAL2A	Cal. estuary	26.6707	−81.8482	2.20	46.5	2.8	2.8	0.5	28.2	3.3	3.3	144.8	11.7	23.2		
E13	CAL3A	Cal. estuary	26.6905	−81.8182	0.51	37.1	2.4	1.3	0.3	50.2	2.1	2.9	136.3	10.2	35.0		
E14	CAL4A	Cal. estuary	26.7215	−81.7308	0.34	55.3	2.5	7.1	1.9	45.8	2.2	3.3	120.9	10.1	31.9		
E15	CAL5A	Cal. estuary	26.4920	−82.0154	32.51	30.7	0.3	1.5	4.7	31.5	28.6	16.6	105.0	37.9	5.5		
E16	CAL6A	Cal. estuary	26.5242	−82.0055	33.17	64.2	0.6	1.0	0.3	21.8	29.4	16.1	131.6	46.4	7.6		
E17	CAL7A	Cal. estuary	26.5299	−81.9726	23.69	134.3	1.4	1.3	1.5	12.1	8.1	6.2	58.8	12.7	7.4		
E18	CAL8A	Cal. estuary	26.5410	−81.9414	16.50	128.2	2.4	2.4	1.1	31.5	18.3	14.6	164.5	32.9	9.3		
E19	CAL9A	Cal. estuary	26.5684	−81.9239	12.02	53.3	2.3	0.4	1.1	43.4	10.4	8.7	174.5	27.7	16.3		
E20	CAL10A	Cal. estuary	26.5887	−81.9065	8.82	36.5	1.9	1.2	0.3	26.7	9.6	9.8	200.5	24.6	15.6		
E21	CAL11A	Cal. estuary	26.6270	−81.8924	5.20	28.7	3.2	<0.05	0.3	30.3	8.7	7.8	194.2	19.6	13.0		
E22	CALFL	Cal. river	26.7228	−81.6960	0.44	137.3	3.2	1.1	5.1	44.3	2.8	3.7	188.6	11.8			
R1	CAL111	Cal. river	26.7211	−81.6922	0.25	391.7	3.2	1.0	2.2	78.9	4.3	5.0	187.2	10.0	13.5		
R2	CAL112	Cal. river	26.7885	−81.3030	0.24	221.1	1.9	1.9	1.8	50.2	3.9	2.6	163.5	13.3	22.3		
R3	CAL113	Cal. river	26.8394	−81.0809	0.11	46.8	3.4	0.6	1.2	65.7	3.8	0.3	28.5	12.6	21.4		
PZ1	CALPZ	Piezometer	26.6905	−81.8182		134.3		5.7	0.8	56.8						1.0	Estuary piezometer
PZ2	CALPZ2	Piezometer	26.5255	−81.9983	30.29	157.5	7.8	1.5	4.8	75.9	121.0	45.5	143.8	142.3		1.0	Estuary piezometer
PZ3	CALPZ3	Piezometer	26.5615	−81.9260	21.34	39.4	8.1	0.6	6.5	39.6	59.9	24.8	223.0	41.6		1.0	Estuary piezometer
GW1	GW101	Monit. well	26.6711	−81.8799	0.37	75.2	4.1	0.6	25.6	47.9	29.5	13.3	98.0	13.6		5.9 (4.3)	Upper surficial
GW2B	GW102	Monit. well	26.5100	−82.0846	32.95	73.6	8.5	<0.05	42.7	152.0	472.6	150.5	890.8	249.7		6.6 (4.9)	Upper surficial
GW2	GW103	Monit. well	26.5100	−82.0846	5.43	34.2	1.9	0.8	21.6	131.7	217.9	30.2	126.8	90.7		6.6 (4.9)	Upper surficial
GW4	GW104	Monit. well	26.5588	−81.8982	0.34	54.8	2.5	0.6	41.5	108.8	68.8	31.9	250.6	41.7		6.6 (4.9)	Upper surficial
GW5	GW105	Monit. well	26.5238	−81.9202	2.46	136.0	3.6	0.4	76.1	130.3	282.9	131.5	164.0	187.6		5.9 (4.6)	Upper surficial
GW6	GW106	Monit. well	26.5185	−81.9357	0.82	56.9	9.4	0.3	67.9	124.0	148.4	54.8	1647.9	81.5		5.9 (5.2)	Upper surficial
GW7	GW107	Monit. well	26.7114	−81.8382	0.32	115.0	35.2	4.6	13.8	45.6	18.1	9.7	150.6	25.7		9.2 (7.9)	Upper surficial
GW8	GW108	Monit. well	26.7158	−81.8072	0.70	163.3	22.6	0.3	11.8	34.2	68.6	54.3	376.5	46.8		5.9 (4.3)	Upper surficial
GW9	GW109	Monit. well	26.7332	−81.7128	0.41	160.6	10.2	0.8	80.6	121.7	67.1	110.6	1432.3	36.3		6.5 (5.2)	Upper surficial
GW10	GW110	Monit. well	26.7346	−81.7309	0.60	187.8	3.0	1.0	24.6	55.4	64.1	49.4	192.3	25.0		6.5 (5.2)	Upper surficial
GW11	GW111	Monit. well	26.7046	−81.6797	0.28	143.9	0.4	0.2	23.3	43.6	31.0	26.2	398.7	20.2		8.9 (6.6)	Upper surficial
GW12	GW112	Monit. well	26.6805	−81.7832	0.23	82.2	1.8	0.3	8.4	36.2	40.7	22.4	152.8	27.3		6.6 (4.9)	Upper surficial
GW13	GW113	Monit. well	26.5238	−81.9202	0.37	183.4	0.2	0.2	5.4	15.1	148.4	4.9	306.2	24.8		101 (NA)	Upper mid. Hawthorne
GW14	GW114	Monit. well	26.3339	−81.8046	2.13	179.9	0.4	0.9	29.4	57.9	130.6	100.2	903.6	74.5		154 (NA)	Lower mid. Hawthorne
GW15	GW115	Monit. well	26.3339	−81.8046	3.54	88.6	0.2	0.1	14.3	60.5		282.9	2731.4	38.5		5.9 (4.6)	Upper surficial
GW16	GW116	Monit. well	26.3339	−81.8046	0.93	102.7	2.8	0.9	39.0	149.4	196.8	21.9	255.3	93.0		39 (NA)	Lower surficial
GW17	GW117	Monit. well	26.3875	−81.8262	0.44	26.8	3.4	0.5	25.0	55.1	175.7	14.4	126.1	122.7		6.9 (4.9)	Upper surficial
GW18	GW118	Monit. well	26.4419	−81.8346	0.24	67.3	0.5	2.5	25.0	51.6	49.1	33.7	273.2	27.5		6.6 (4.9)	Upper surficial

Table 3
April 2010 nutrient concentrations and radium activities from the Caloosahatchee River Estuary groundwater study.

Station ID	WHOI ID	Sample type	Latitude (°N)	Longitude (°W)	Salinity	SiO_4^-	PO_4^{3-}	$NO_3^- + NO_2^-$	NH_4^+	TDN	^{224}Ra	^{223}Ra	^{226}Ra	^{228}Ra	Water age (days)	Monitoring well depth (m)*	Aquifer formation
						(μmol L^{-1})					(dpm 100 L^{-1})						
E23	CAL 200	Cal. estuary	26.4867	−82.0171	20.73	7.8	0.3	0.7	3.0	13.8	23.0	14.9	123.2	39.8	8.8		
E24	CAL 201	Cal. estuary	26.5052	−82.0177	14.95	5.2	0.2	0.4	2.5	12.2	16.6	11.9	128.1	29.3	9.0		
E25	CAL 202	Cal. estuary	26.5293	−81.9879	8.91	9.8	0.4	3.1	4.5	21.4	13.5	10.0	128.1	24.3	9.4		
E26	CAL 203	Cal. estuary	26.5294	−81.9873	5.13	11.0	0.3	1.8	3.4	19.0	9.7	6.0	123.7	14.4	6.8		
E27	CAL 204	Cal. estuary	26.5878	−81.9092	2.43	47.8	1.8	5.0	5.1	38.1	7.4	4.2	114.1	12.9	9.0		
E28	CAL 205	Cal. estuary	26.6488	−81.8754	0.43	99.5	1.1	16.4	4.6	71.9	5.6	3.0	131.3	10.5	9.9		
E29	CAL 206	Cal. estuary	26.6860	−81.8293	0.35	98.0	1.3	7.6	3.9	51.5	6.0	4.2	178.2	12.4	11.5		
E30	CAL 207	Cal. estuary	26.6970	−81.7968	0.32	112.5	0.9	16.7	4.6	77.3	4.9	4.1	190.2	16.1	21.6		
E31	CAL 208	Cal. estuary	26.7166	−81.7636	0.31	98.9	1.0	12.5	4.2	66.8	4.6	4.2	160.5	13.4	18.6		
E32	CAL 209	Cal. estuary	26.7220	−81.7268	0.28	114.6	1.2	13.6	5.3	79.4	5.0	3.3	143.6	13.1	16.3		
E33	CAL 210	Cal. estuary	26.7229	−81.6960	0.26	86.5	1.8	9.0	4.1	63.2	3.9	2.3	145.5	15.4	27.2		
R1	CAL 211	Cal. river	26.7220	−81.6906	0.26	55.2	1.6	17.3	12.5	85.4	4.3	3.3	146.1	16.8	26.7		
PZ4	CAL 212	Piezometer	26.5260	−81.9561	20.36	28.4	3.6	4.3	44.4	58.7	1158.7	959.1	9945.4	900.9		2.0	Estuary piezometer
PZ5	CAL 213	Piezometer	26.5260	−81.9561	16.97	23.5	1.1	2.0	34.0	52.7	1418.6	182.0	8532.4	1275.4		1.0	Estuary piezometer
PZ6	CAL 214	Piezometer	26.5260	−81.9561	17.61	38.9	2.4	0.4	35.7	56.9	558.8	77.9	2244.9	463.4		0.5	Estuary piezometer
PZ7	CAL 215	Piezometer	26.5425	−81.9522	8.32	12.9	0.8	0.5	15.6	26.4	71.2	89.9	113.1	28.6		0.5	Estuary piezometer
PZ8	CAL 216	Piezometer	26.5425	−81.9522	7.56	25.6	1.9	7.5	25.7	51.2	100.3	81.1	150.3	34.5		0.8	Estuary piezometer
GW2B	GW202	Monit. well	26.5097	−82.0846	32.36	110.5	5.3	1.5	59.7		661.3	269.2	1100.2	301.1		6.6 (4.9)	Upper surficial
GW3	GW203	Monit. well	26.6397	−81.8689	0.27	75.8	1.0	0.5	7.7	24.6	52.0	19.7	441.6	42.4		8.2 (6.6)	Upper surficial
GW5	GW 205	Monit. well	26.5238	−81.9202	2.75	78.7	0.3	1.3	21.0	35.7	153.9	62.5	1155.6	148.5		5.9 (4.6)	Upper surficial
GW6	GW206	Monit. well	26.5185	−81.9357	1.05	74.4	6.0	1.0	30.6	52.4	108.8	48.1	2257.3	97.8		5.9 (5.2)	Upper surficial
GW9	GW209	Monit. well	26.7332	−81.7128	0.42	102.4	6.2	2.8	43.8	66.5	47.1	63.7	1141.9	32.3		6.5 (5.2)	Upper surficial
GW10	GW210	Monit. well	26.7346	−81.7309	0.58	217.0	2.5	0.3	12.1	67.4	38.1	7.5	93.4	14.8		6.5 (5.2)	Upper surficial
GW11	GW211	Monit. well	26.7046	−81.6797	0.33	100.6	0.1	2.9	14.9	31.2	23.2	16.1	519.8	19.3		8.9 (6.6)	Upper surficial
GW13	GW 213	Monit. well	26.5238	−81.9202	0.38	218.9	0.3	1.2	9.9	20.2	8.5	4.3	311.2	34.4		101 (NA)	Upper mid. Hawthorne

Please cite this article as: Charette, M.A., et al., Submarine groundwater discharge in a river-dominated Florida estuary, Mar. Chem. (2013), http://dx.doi.org/10.1016/j.marchem.2013.04.001

Table 4
October 2010 nutrient concentrations and radium activities from the Caloosahatchee River Estuary groundwater study.

Station ID	WHOI ID	Sample type	Latitude (°N)	Longitude (°W)	Salinity	SiO_4^- (μmol L^{-1})	PO_4^{3-}	$NO_3^- + NO_2^-$	NH_4^+	TDN	^{224}Ra (dpm 100 L^{-1})	^{223}Ra	^{226}Ra	^{228}Ra	Water age (days)	Monitoring well depth (m)*	Aquifer formation
E34	CAL 301	Cal. estuary	26.4877	−82.0157	31.41	19.2	0.4	0.5	2.2	22.8	33.3	3.3	127.1	59.0	9.1		
E35	CAL 302	Cal. estuary	26.5267	−81.9970	26.89	29.5	0.5	0.8	2.1	22.5	37.5	17.2	172.6	54.6	6.6		
E36	CAL 303	Cal. estuary	26.5315	−81.9599	17.88	42.4	1.0	2.1	4.0	26.8	23.9	6.8	249.4	45.7	10.3		
E37	CAL 304	Cal. estuary	26.5674	−81.9239	14.14	31.6	0.8	3.9	7.8	31.6	16.2	6.5	281.6	42.3	15.9		
E38	CAL 305	Cal. estuary	26.6035	−81.9003	10.45	60.4	1.0	1.4	3.1	32.5	7.7	6.1	286.0	33.8	30.5		
E39	CAL 306	Cal. estuary	26.6471	−81.8744	9.42	51.7	1.7	1.5	2.7	23.8	13.0	12.2	358.4	40.4	20.0		
E40	CAL 307	Cal. estuary	26.6724	−81.8463	5.61	56.0	0.9	4.0	4.5	28.3	13.5	11.4	381.2	34.9	15.7		
E41	CAL 308	Cal. estuary	26.6978	−81.7972	4.04	93.5	0.8	3.4	3.8	25.6	4.9	5.3	375.6	33.2	50.0		
E42	CAL 309	Cal. estuary	26.7164	−81.7618	2.91	69.0	0.9	6.0	5.4	35.5	4.4	3.5	328.6	32.1	53.7		
E43	CAL 310	Cal. estuary	26.7215	−81.7326	3.07	75.9	0.9	4.4	5.2	33.1	6.7	4.5	338.8	29.3	30.2		
E35	CAL 311	Cal. estuary	26.7226	−81.6957	3.39	126.0	1.3	7.2	6.6	40.0	6.9	3.0	345.6	28.0	27.9		
R1	CAL 312	Cal. river	26.7218	−81.6913	0.29	186.0	0.6	15.2	3.5	68.5	3.8	4.5	231.5	13.6	23.7		
PZ9	CAL 313	Piezometer	26.5260	−81.9562	18.41	37.4	8.0	1.1	38.5	56.8	242.5	54.8	5853.2	535.4		1.5	Estuary piezometer
PZ10	CAL 314	Piezometer	26.5260	−81.9562	27.32	30.8	3.5	7.8	27.7	48.4	2295.0	120.1	22545.3	2966.6		1.0	Estuary piezometer
PZ11	CAL 315	Piezometer	26.5260	−81.9562	15.35	84.3	6.3	3.8	54.6	73.6	374.7	35.7	4034.4	382.8		0.3	Estuary piezometer
PZ12	CAL 316	Piezometer	26.5425	−81.9522	13.34	101.0	3.0	0.9	10.1	23.4	134.9	79.4	228.2	53.1		0.5	Estuary piezometer
PZ13	CAL 317	Piezometer	26.5425	−81.9522	8.04	265.0	6.2	0.8	24.7	36.1	134.3	77.0	184.6	53.7		0.5	Estuary piezometer
GW2	GW 302	Monit. well	26.5097	−82.0846	4.46	102.0	0.9	26.3	118.0	236.2	121.9	17.8	110.0	30.1		6.6 (4.9)	Upper surficial
GW2B	GW 302B	Monit. well	26.5097	−82.0846	40.25	121.0	6.4	3.7	123.0	185.2	432.3	128.3	1032.4	263.8		6.6 (4.9)	Upper surficial
GW3	GW 303	Monit. well	26.6397	−81.8689	0.18	51.5	1.4	17.5	31.0	82.9	13.6	6.7	334.4	28.7		8.2 (6.6)	Upper surficial
GW5	GW 305	Monit. well	26.5238	−81.9202	2.57	179.0	30.1	0.8	84.2	115.6	180.0	46.8	1313.1	179.6		5.9 (4.6)	Upper surficial
GW6	GW 306	Monit. well	26.5185	−81.9357	1.01	51.2	10.6	0.5	44.9	62.2	81.4	26.3	1884.9	87.2		5.9 (5.2)	Upper surficial
GW9	GW 309	Monit. well	26.7332	−81.7128	0.57	229.0	5.5	0.1	49.5	63.4	40.0	109.9	2456.8	54.2		6.5 (5.2)	Upper surficial
GW10	GW 310	Monit. well	26.7346	−81.7309	0.57	320.0	2.2	1.4	33.3	62.5	6.7	13.4	167.5	46.2		6.5 (5.2)	Upper surficial
GW11	GW 311	Monit. well	26.7046	−81.6797	0.29	221.0	0.4	0.2	27.9	37.9	22.1	14.6	589.8	33.4		8.9 (6.6)	Upper surficial
GW13	GW 313	Monit. well	26.5238	−81.9202	0.38	291.0	0.2	0.1	18.0	20.7	14.3	4.3	386.7	30.4		101 (NA)	Upper mid. Hawthorne

Please cite this article as: Charette, M.A., et al., Submarine groundwater discharge in a river-dominated Florida estuary, Mar. Chem. (2013), http://dx.doi.org/10.1016/j.marchem.2013.04.001

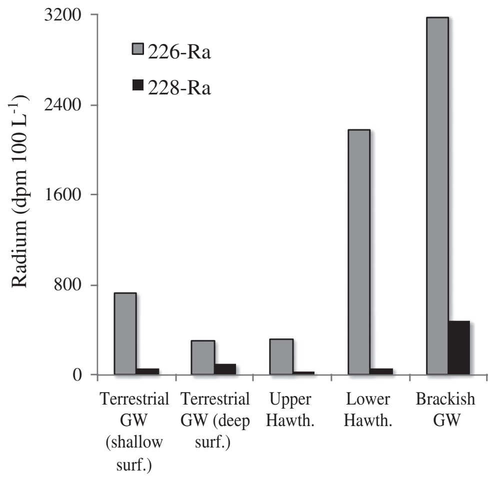

Fig. 3. Average ^{226}Ra and ^{228}Ra activities in different potential groundwater sources for the estuary. The averages include data from all four time periods. The average salinity of the "brackish" groundwater samples was 20. All other groundwater samples have a salinity <3.

The short-lived Ra isotopes, ^{223}Ra, and ^{224}Ra, averaged 51.0 and 107 dpm 100 L^{-1} in all groundwater wells and piezometers, respectively. There was no statistically significant difference between seasons. The ^{224}Ra/^{228}Ra activity ratio in groundwater, used to derive estuarine water mass ages, averaged 1.54 ± 0.97. Samples averaged according to groundwater source were largely similar with one exception: terrestrial groundwater samples from the shallow surficial aquifer had an average ^{224}Ra/^{228}Ra ratio of 1.35. All other groundwater sources (brackish, Hawthorne aquifer) had higher averages ranging from 1.7 to 1.9.

3.2. Surface water radium

Samples for radium were collected from the Gulf of Mexico, through the estuary salinity gradient, and along the Caloosahatchee River to its origin at Lake Okeechobee. Radium-226 activities in surface water samples were only a factor of 4–9 times lower than average groundwater, which suggests that significant groundwater–surface water exchange was occurring (Tables 1–4). Unlike groundwater, there was significant seasonal and interannual variability in ^{226}Ra both within the estuary and in the Gulf of Mexico endmember. The average estuarine ^{226}Ra for April-09, Oct-09, April-10, and Oct-10 was 341, 160, 153, and 297 dpm 100 L^{-1}, respectively. These values are consistent with a ^{226}Ra activity range of ~150 to 500 dpm 100 L^{-1} for the Charlotte Harbor estuarine system less than 20 km to the north of our study site (Miller et al., 1990). The ^{226}Ra activity in our outermost Gulf of Mexico stations ranged from 22 to 55 dpm 100 L^{-1}. The average estuarine ^{228}Ra/^{226}Ra for April-09, Oct-09, April-10, and Oct-10 was 0.18, 0.16, 0.13, and 0.13, respectively.

In the freshwater reaches (salinity <1), ^{226}Ra ranged from 6.3 to 231 dpm 100 L^{-1} and averaged 132 dpm 100 L^{-1}, significantly higher than the typical river endmember. For example, in the Hudson River estuary, Li and Chan (1979) reported a river ^{226}Ra average of ~1 dpm 100 L^{-1}. Krest et al. (1999) found Mississippi River ^{226}Ra activities in the range of ~10–15 dpm 100 L^{-1}. In our dataset, the lowest freshwater ^{226}Ra (6.6–29 dpm 100 L^{-1}) were found in Lake Okeechobee, which we sampled twice during 2009. ^{226}Ra generally increased with increasing distance toward the Franklin Lock (not shown). Particulate ^{226}Ra, measured on suspended solids in April 2009 on the landward side of the Franklin Lock, was 1.7 dpm 100 L^{-1}, less than 0.5–1% of the average estuarine ^{226}Ra.

The remaining three Ra isotopes, ^{228}Ra, ^{223}Ra, and ^{224}Ra averaged 30.7, 9.18, and 13.2 dpm 100 L^{-1} in all surface water samples, respectively. Radium-228 generally tracked ^{226}Ra, though the short-lived Ra isotopes were more variable due largely to differences in estuarine residence time, which is discussed in more detail below.

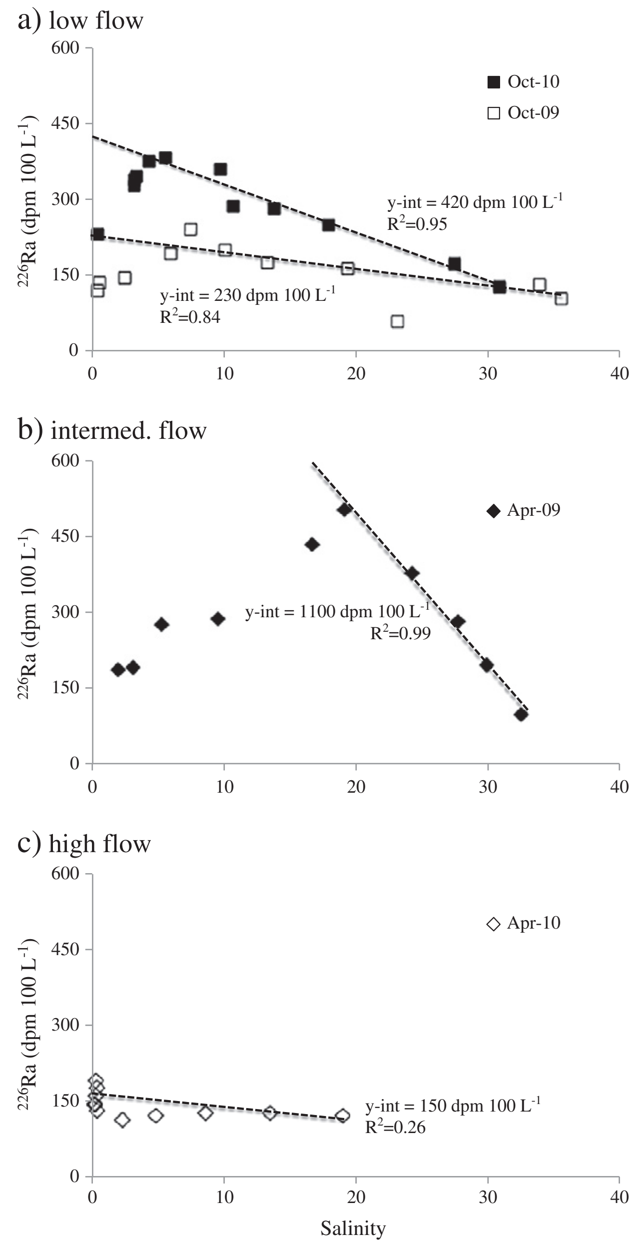

Fig. 4. Radium-226 distribution with salinity for the four sampling periods sorted according to (a) low, (b) intermediate, and (c) high flow originating from the S-79 control structure (Franklin Lock) for 2.5 weeks prior to our sampling period. Also shown is a linear curve fit, y-intercept and R^2 for the conservative portion of the estuarine ^{226}Ra distribution.

4. Discussion

Within the estuary, ^{226}Ra and ^{228}Ra displayed a typical non-conservative distribution with salinity (Figs. 4 and 5). Within the estuarine mixing zone, ^{226}Ra peaked at salinities less than 10 for the two October sampling periods while in April 2009 ^{226}Ra peaked at a salinity of ~20; the April 2010 distribution was generally flat throughout the entire estuary. This non-conservative Ra behavior has been observed for many riverine systems (e.g. Moore, 1997), though it was generally believed that the low salinity peak was due to ^{226}Ra desorption from particles (e.g. Li and Chan, 1979). After peak values were reached, ^{226}Ra generally followed a conservative mixing line with the Gulf of Mexico

ARTICLE IN PRESS

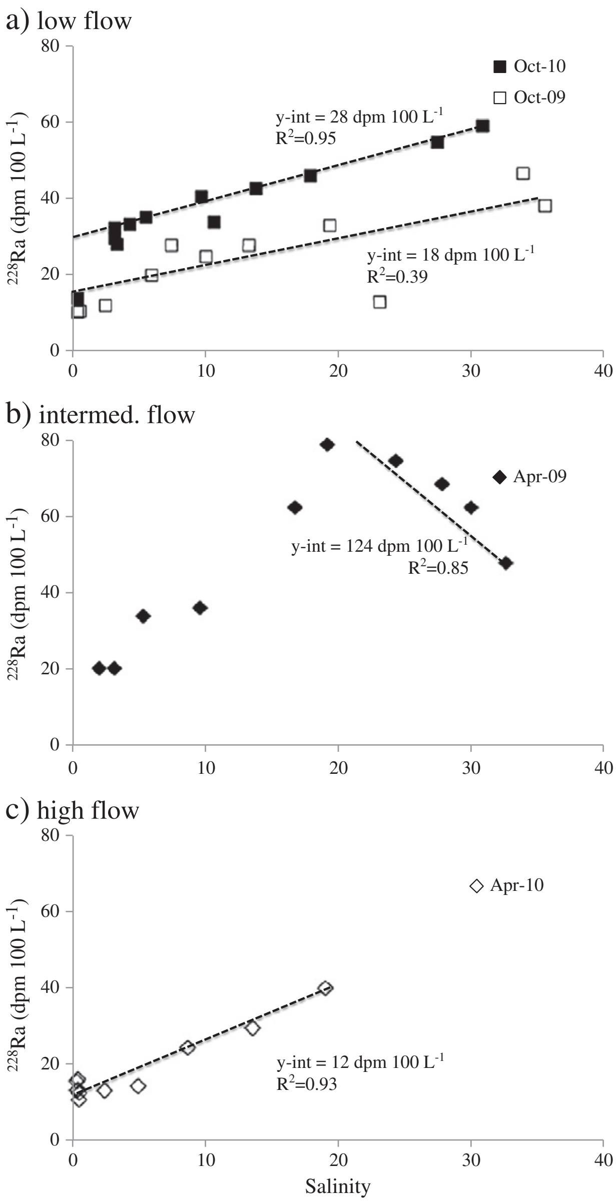

Fig. 5. Radium-228 distribution with salinity for the four sampling periods sorted according to (a) low, (b) intermediate, and (c) high flow originating from the S-79 control structure (Franklin Lock) for 2.5 weeks prior to our sampling period. Also shown is a linear curve fit, y-intercept and R^2 for the conservative portion of the estuarine ^{228}Ra distribution.

endmember for all seasons. Radium-228 displayed a similar trend to ^{226}Ra, with one major exception: the Gulf of Mexico ^{228}Ra endmember was always higher than the river endmember. Trend lines for Figs. 4 and 5 use the conservative mixing portion of the Ra distribution to compute an effective freshwater endmember for each of the time periods sampled. These y-intercept values were highest for both isotopes in April 2009 and October 2010, and lowest for April 2010. These values are well above the measured particulate ^{226}Ra activity of 1.7 dpm 100 L^{-1}; hence even if 100% of the particulate ^{226}Ra desorbed upon entering the estuary, it could account for <1% of the ^{226}Ra increase.

We conclude that the Ra distribution is largely driven by a combination of the Franklin Lock discharge history leading up to our sampling trip and the amount of Ra delivered to the estuary via SGD. Regarding river fluxes, the Ra data are grouped according to the discharge from Franklin Lock in the 2.5 weeks prior to sampling (time-scale roughly equal to the average estuarine water residence time). Under high flow (Figs. 4c and 5c), the Ra distribution was relatively flat due to river Ra

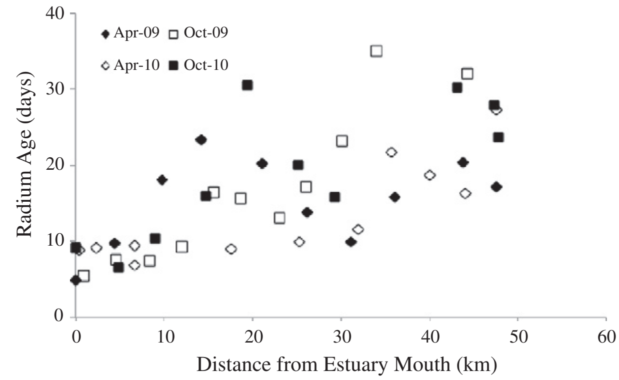

Fig. 6. Radium derived water mass ages in the estuary for the four sampling periods as a function of distance from the Franklin Lock dam.

activities dominating throughout the estuary. Lock discharges were above average both during and several weeks prior to our sampling trip. Under low flow, ^{226}Ra peaked at relatively low salinity (Fig. 4a) while ^{228}Ra peaked at high salinity due to the high ^{228}Ra/^{226}Ra of tidally flushed Gulf of Mexico water (Fig. 5a). In both low flow cases, October 2009 and 2010, there were no water releases from the lock during the sampling expedition, and none 3 days prior to the start of the October 2010 trip (Fig. 2a). In April 2009 (intermediate flow, Figs. 4b and 5b), while there was no lock discharge during our trip, there had been a moderate freshwater release just 3 days prior. This transient release is reflected in ^{226}Ra and ^{228}Ra peaks at intermediate-high salinity.

4.1. Estuarine water residence times derived from radium isotopes

Knowledge of water residence time (T_w) is required for quantifying radium sources and sinks within the estuary and ultimately submarine groundwater discharge. The large-scale input of radium isotopes along the coastline and the boundaries of estuaries is similar to a purposeful tracer release, with the short-lived radium isotopes providing the rate of dispersion based on their decay as they mix away from the source. Both residence time and age are used interchangeably to describe how long water remains in an estuary. One definition of residence time is "the time it takes for any water parcel to leave a given water body through its outlet to the sea", usually relative to an arbitrary reference point within the system (Monsen et al., 2002). On the other hand, age is defined as the time a water parcel has spent since entering the

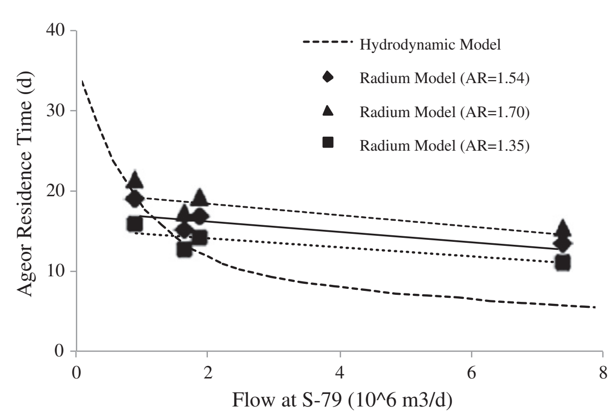

Fig. 7. Estuarine residence time or average age derived from a hydrodynamic model (Qiu and Sun, 2009; 20% e-folding time model) or Ra isotopes plotted as a function of discharge at the S-79 control structure (Franklin Lock). The Ra model ages are for the four time periods covered by this study and were derived from a range of assumptions regarding the groundwater endmember ^{224}Ra/^{228}Ra activity ratio (AR). Curve fits for the three Ra models are linear and each had an $R^2 = 0.68$.

Please cite this article as: Charette, M.A., et al., Submarine groundwater discharge in a river-dominated Florida estuary, Mar. Chem. (2013), http://dx.doi.org/10.1016/j.marchem.2013.04.001

estuary through one of its boundaries, defined for Ra isotopes with the following equation (Moore et al., 2006):

$$T_w = \frac{\left[F\left({}^{224}Ra/{}^{228}Ra\right) - I\left({}^{224}Ra/{}^{228}Ra\right)\right]}{I\left({}^{224}Ra/{}^{228}Ra\right)\lambda_{224}}$$

In this case F(^{224}Ra/^{228}Ra) is the ^{224}Ra/^{228}Ra activity ratio (AR) of the input into the system and I(^{224}Ra/^{228}Ra) is the ^{224}Ra/^{228}Ra AR of the estuarine sample. The decay constant for ^{224}Ra is represented as λ_{224}. The application of this model requires precise knowledge of the ^{224}Ra/^{228}Ra AR of input, which in this case was derived from the average ratio measured in groundwater along the estuary boundary.

Using a F(^{224}Ra/^{228}Ra) value of 1.54, we derived estuarine water ages as a function of distance from the Franklin Lock (Fig. 6). In general, age increased with distance along the estuary axis for all seasons. However, average estuarine age did vary with season, ranging from a low of 13.5 days in April 2010 to a high of 19.0 days for October 2010. Age was inversely correlated with discharge from the Franklin Lock averaged over a time scale similar to our estuarine age estimates (2.5 weeks) (Fig. 7), suggesting that freshwater releases from the lock may exert a significant control on the flushing time of the system.

This is consistent with the findings of Qiu and Sun (2009), who examined the residence time of the Caloosahatchee estuary with a hydrodynamic model that included the combined effects of Franklin Lock discharge and tides. They noted that, while tides had an influence on residence time near the estuary mouth, discharge at S-79 was the main driver of estuarine flushing for this system. In April 2010, when discharge at S-79 was high, their model produced an estuarine transit time of 7.4 days, approximately half our Ra-based estimate (Fig. 7). In October 2010, when discharge was at a minimum, their model produced an estimate of 19.1 days, in excellent agreement with our Ra age of 19.0 days. Hence, our two methods appear to agree quite well under low flow conditions, with increasing divergence as Franklin Lock discharges increase. Since we integrated the Franklin Lock discharge over the 2.5 weeks preceding our study, we examined whether or not a shorter or longer time scale would produce an age vs. flow relationship more in line with the model. However, we found that divergence in the two approaches was essentially the same at high discharge for a range in discharge integration time scales from one week to one month.

We also examined the effect of different F(^{224}Ra/^{228}Ra) assumptions using the terrestrial surficial groundwater average of 1.35 (which lowered the average ages by 16–17%) and the brackish groundwater average of 1.70 (which increased the average ages by 13–14%). The agreement was slightly better at the intermediate lock discharge values but still divergent at the higher flow rates. Alternatively, the model divergence could be due to an underestimate of the return flow at the estuary mouth in the model, or inclusion of "old" Gulf of Mexico water in the return flow in terms of Ra age. These differences can be attributed to the fact that such hydrodynamic models (by design)

4.2. Sources of radium isotopes to the estuary other than groundwater

In order to evaluate the relative importance of Ra sources to the estuary, we must first calculate the net Ra flux from the estuary. At steady-state, this flux is equivalent to $[(A-A_{GoM})/T_{w}]$ where A is the average Ra activity in the estuary and A_{GoM} is the offshore endmember (Gulf of Mexico). For ^{226}Ra, this flux ranged from a low of 0.84×10^{10} dpm d^{-1} in April 2010 to 2.8×10^{10} dpm d^{-1} in April 2009. These values are on the order of ~10% of the Mississippi River total ^{226}Ra flux as reported by Krest et al. (1999) despite a greater than 2-orders of magnitude difference in the freshwater flux between the two systems. This difference is most likely explained by the high input of ^{226}Ra via SGD and the aquifer lithology.

While we were not able to perform sediment core incubations to quantify the benthic diffusive flux, it is likely a small component of the overall radium mass balance for the system. Using a flux rate for sediment diffusion of ^{226}Ra from Veeh et al. (1995) (0.036 dpm m^{-2} d^{-1}) and an estuarine surface area of 5.55×10^7 m^2, we derived a ^{226}Ra exchange rate of 2.0×10^6 dpm d^{-1} or approximately 0.01–0.02% of the total ^{226}Ra flux. Using an average sediment flux ^{226}Ra rate from the Charlotte Harbor study (0.7 dpm m^{-2} d^{-1}), the non-SGD derived benthic flux becomes 0.14–0.50% of the total ^{226}Ra flux (Miller et al., 1990). Hence, diffusion from sediments is a negligible source of ^{226}Ra to the estuary.

Desorption from suspended sediments is also estimated to be a small contribution to the total flux. From the product of our particulate ^{226}Ra activity of 1.7 dpm 100 L^{-1} and the freshwater release through the Franklin Lock, we derived a potential ^{226}Ra flux to the dissolved pool from suspended particle desorption. Calculated for each time point and assuming that all ^{226}Ra desorbed from particles upon entering the estuarine mixing zone, this potential source ranged from 1.5 to 8.9×10^7 dpm d^{-1} or 0.08–0.76% of the total ^{226}Ra flux. For the Peace River to the north, Miller et al. (1990) found that suspended sediments would release at most 4 dpm 100 L^{-1} ^{226}Ra and concluded that this process was grossly inadequate to explain the range of activities in the downstream Charlotte Harbor.

In contrast to the particulate flux, the dissolved ^{226}Ra flux from the freshwater releases at the Franklin Lock is a more substantial component of the ^{226}Ra mass balance for the estuary. The river ^{226}Ra flux, a product of ^{226}Ra measured on the freshwater side of the lock and the 2.5-week average discharge at the time of sampling, ranged from 0.55 to 2.1×10^9 dpm d^{-1}. This represented as little as 3% of the total Ra flux for April 2009 or as much as 66% of the budget for April 2010. Therefore, while discharges from the lock are a source of ^{226}Ra to the estuary that must be accounted for, sediment diffusion and desorption from particles (combined flux ~2%) can be neglected.

For ^{228}Ra, we assume that the desorbable particulate flux is negligible because it was not detected in our large volume particulate sample. Regarding benthic diffusion, given the faster regeneration rate of ^{228}Ra relative to ^{226}Ra, it has the potential to be more important for ^{228}Ra. However, Miller et al. (1990) found that the benthic ^{228}Ra flux was only three times higher than ^{226}Ra; hence, we assume that it is also a negligible ^{228}Ra source for our system.

4.3. Radium isotope mixing model for quantifying SGD fluxes to the estuary

There are several lines of evidence that support multiple radium sources for the Caloosahatchee River estuary. These are best discussed in the context of ^{226}Ra and ^{228}Ra mixing diagrams for the four sampled time periods (Fig. 8a–d). For all seasons sampled, except for April 2010 when river discharge was high, no two sources alone can explain the average activities of both long-lived Ra isotopes within the estuarine mixing zone. The Gulf of Mexico endmember is ^{228}Ra enriched while the river is ^{228}Ra depleted relative to ^{226}Ra. For example, during the period with low discharge at Franklin Lock (October 2010, Fig. 8d), the estuary average ^{226}Ra and ^{228}Ra plots well above the mixing line between the river and Gulf of Mexico endmembers. Furthermore, the estuary is variably enriched in ^{228}Ra relative to ^{226}Ra (activity ratios = 0.13–0.18) on a seasonal basis such that excess Ra cannot be supplied by either terrestrial surficial aquifer groundwater or brackish groundwater alone.

Having multiple tracers of groundwater provenance allows for the solution of a mixing model to constrain the fraction of each source that supplied radium to the estuary during a given measurement

Please cite this article as: Charette, M.A., et al., Submarine groundwater discharge in a river-dominated Florida estuary, Mar. Chem. (2013), http://dx.doi.org/10.1016/j.marchem.2013.04.001

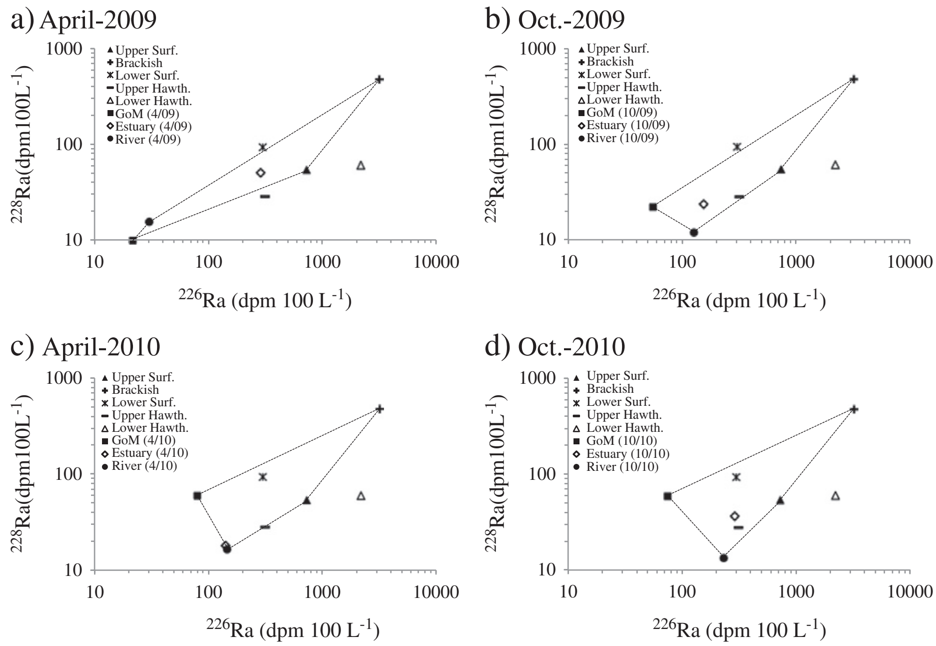

Fig. 8. Radium-226 and ^{228}Ra for groundwater and surface water endmembers relative to average estuarine activities for the four time periods. The lines illustrate the boundaries for the four endmember mixing model.

period. The model involves a series of equations with four unknowns (the four radium sources to the estuary):

$$f_r + f_{GoM} + f_{ter} + f_{mgw} = 1$$
$$S_r \times f_r + S_{GoM} \times f_{GoM} + S_{ter} \times f_{ter} + S_{mgw} \times f_{mgw} = S_{CRE}$$
$$^{226}Ra_r \times f_r + {}^{226}Ra_{GoM} \times f_{GoM} + {}^{226}Ra_{ter} \times f_{ter} + {}^{226}Ra_{mgw} \times f_{mgw} = {}^{226}Ra_{CRE}$$
$$^{228}Ra_r \times f_r + {}^{228}Ra_{GoM} \times f_{GoM} + {}^{228}Ra_{ter} \times f_{ter} + {}^{228}Ra_{mgw} \times f_{mgw} = {}^{228}Ra_{CRE}$$

where f = endmember fraction, r = river, GoM = Gulf of Mexico, ter = terrestrial groundwater, mgw = marine (brackish) groundwater, CRE = Caloosahatchee River estuary, and S = salinity. For this model, the endmember concentrations for the tracers must be defined (Table 5). In the case of the terrestrial groundwater, we assume that this can be represented by the average of all low salinity samples from the shallow unconfined aquifer (Fig. 3). For the river values, we used the measured values on the landward side of Franklin Lock. For the Gulf of Mexico values, we used the measured offshore endmember for the 2009 samples. In 2010, we did not have stations outside the estuary so we used the curve fits in Figs. 4 and 5 to predict the ^{228}Ra and ^{226}Ra activities at salinity = 36. For marine groundwater, we used the brackish groundwater average values shown in Fig. 3 (far right). The average salinity of our brackish groundwater samples was 20.

We used an optimum multiparameter approach within MATLAB to solve for f_r, f_{GoM}, f_{ter}, and f_{mgw} for each of the four time periods. The approach is a least squares (non-negative) best fit of the dataset. The model resulted in relatively high SGD fractions during two periods: April 2009 and October 2010 (Fig. 9, "avg. EM" case) when freshwater releases from the Franklin Lock were relatively low. Intermediate SGD fractions were observed for October 2009 (intermediate lock discharge) and very low SGD fractions were predicted for April 2010 (the highest lock discharge of the four periods). In terms of the relative contribution of terrestrial (f_{ter}) vs. brackish (f_{mgw}) groundwater, brackish groundwater dominated in April 2009 ($f_{ter} = 0$), while terrestrial groundwater dominated in all other seasons. Leading up to this period, groundwater levels were rapidly rising (Fig. 2b) whereas the groundwater levels were relatively stable (April 2010) or falling (both October time periods). This seasonal pattern could be explained by rising groundwater levels leading to a flushing of stored marine groundwater from the aquifer into the estuary (April 2009) and rapidly decreasing groundwater levels releasing stored terrestrial groundwater (October periods) (Michael et al., 2005; Charette, 2007).

To test the sensitivity of the model to endmember assumptions, we conducted a separate model run where we increased the groundwater averages by 50% (Fig. 9, "high EM" case). We fixed the river and GoM values in both cases as the model is fairly insensitive to changes in their values within uncertainty. In general, the use of 50% higher than average groundwater Ra activities served to lower the overall contribution of total SGD ($f_{ter} + f_{mgw}$) to the estuarine water column. In one case (Oct-09), the different assumptions led to not only a decrease in the total SGD fraction, but also a shift from mostly terrestrial SGD (avg. endmember case) to mostly brackish groundwater (high endmember case).

An example of the station-by-station model output for the October 2010 estuarine data is shown in Fig. 10. In the 30 km from the estuary mouth, f_{GoM} decreased from >80% of the total volume to <20%. In the

Table 5
Endmember salinity and radium isotope activities (dpm 100 L^{-1}) used in the mixing model.

	Gulf of Mexico			River					
	Apr-09	Oct-09	Apr,Oct-10	Apr-09	Oct-09	Apr-10	Oct-10	Marine GW	Terr. GW
Salinity	36.50	35.39	36.00	0.25	0.25	0.25	0.25	20.00	0.75
^{226}Ra	22.1	55.0	60.0	230	180	146	230	3200	725
^{228}Ra	9.4	22.0	50.0	15.0	11.7	16.8	14.0	475	55.0

Please cite this article as: Charette, M.A., et al., Submarine groundwater discharge in a river-dominated Florida estuary, Mar. Chem. (2013), http://dx.doi.org/10.1016/j.marchem.2013.04.001

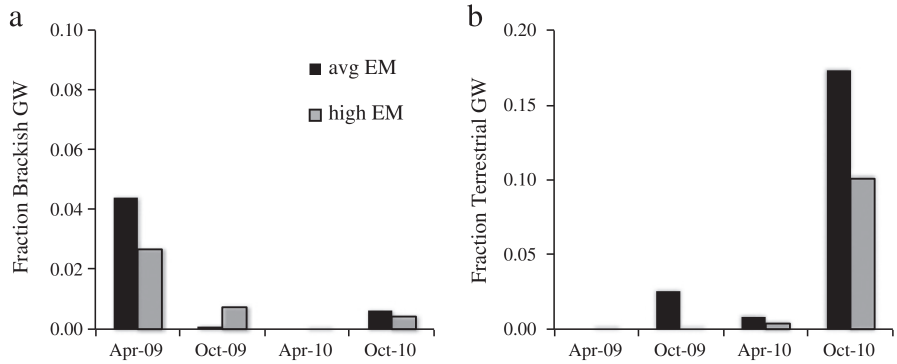

Fig. 9. Mixing model sensitivity analysis for the (a) brackish and (b) terrestrial groundwater fractions. The model was run for two different scenarios: average endmember (EM) and high EM (150% of average).

upper half of the estuary, f_{ter} comprised 20–30% of the estuary volume except for a single station at 40 km from the mouth where it decreased to <5%. This decrease was balanced by an increase in f_r, likely related to the often observed episodic releases of water releases from Franklin Lock working their way down the estuary. In this example, only a small fraction of marine groundwater was detected at each station.

We can use the mixing model results (average groundwater endmember case) and the Ra-derived average estuarine water mass age to derive the volumetric SGD flux to the estuary (e.g. $SGD_{ter} = [(f_{ter} \times V_{CRE})/T_w]$, where V_{CRE} = the volume of the estuary). SGD rates ranged from a low of 8.5×10^4 m^3 d^{-1} in April 2010 to a high of 1.3×10^6 m^3 d^{-1} in October 2010 for the Caloosahatchee River estuary (Table 6). These estimates compare well with a seasonal study of SGD (Ra-derived) for the similarly sized Peace (0.43–2.5 $\times 10^5$ m^3 d^{-1}) and Myakka (0.43–3.9 $\times 10^5$ m^3 d^{-1}) River estuaries (Miller et al., 1990). In April 2009, terrestrial SGD was 44% of the total SGD, compared with 98–100% for the other three time periods (the terrestrial SGD fluxes were adjusted to reflect the fact that the brackish groundwater endmember had a salinity of 20 and therefore includes 45% freshwater/55% seawater). For the four time periods, these fluxes ranged from 2 to 140% of the river discharge through Franklin Lock integrated over the 2.5 weeks prior to our study. When normalized to the area of the estuary, SGD rates ranged from 0.15 to 2.3 cm d^{-1}. These values are low compared with radon-based estimates of SGD at stations in the upper (5.7 ± 6.4 cm d^{-1}) and lower river (12.3 ± 21.9 cm d^{-1}) recorded in March 2009 (Reich, 2009). However, this is not entirely unexpected as our normalized values assume that SGD is uniformly distributed across the estuary bottom when in reality it is likely focused within a relatively narrow band along the estuary margin (Mulligan and Charette, 2006).

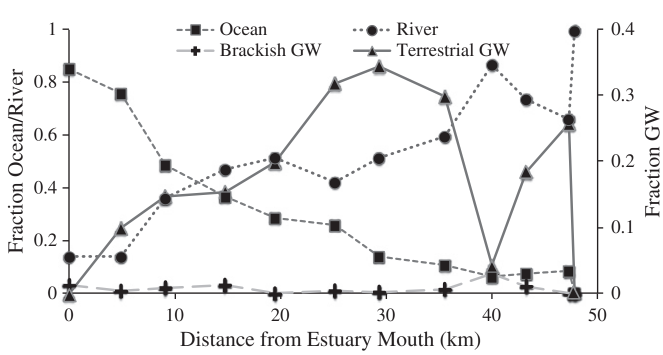

Fig. 10. Results of the four endmember mixing model for October 2010. The source water fractions are plotted for each station within the estuary as a function of the station distance from the estuary mouth.

Also, if we used the estuarine residence time values from the hydrodynamic model, our SGD fluxes would increase by 130–150% for April and October 2009 and 340% for April 2010. For October 2010, where the Ra and model ages were similar, the SGD estimate would remain largely unchanged.

These specific discharge rates are comparable to those reported in a study on Tampa Bay (0.22–1.45 cm d^{-1}), estimated with a nearly identical ^{226}Ra mass balance approach (Swarzenski et al., 2007). Using a radon mass balance approach for the west Florida Shelf off Tampa, Smith and Swarzenski (2012) reported SGD rates that varied between 2.5 and 15 cm d^{-1}. Our SGD estimates are on the low end compared to those derived from seepage meter and radon measurements in the Indian River Lagoon estuary (1.5–116 cm d^{-1}) located along the east coast of Florida (Martin et al., 2007). Again, since the Martin et al. study used point measurements of SGD, and our model assumes uniform distribution, such disagreement should not be entirely unexpected for reasons outlined above.

As an independent check on our SGD estimates, we constructed a simple water balance for the watershed. The water balance was based on the product of average daily rainfall (m/d) for the year preceding the study (e.g. for April 2009, we averaged rainfall from April 2008 to April 2009), the watershed area (m^2), and evapotranspiration (here we used 0.7, typical for southern Florida; Abtew, 2004; Jiang et al., 2009). We then assumed that this net recharge value must be balanced by loss to the estuary. This calculation returned values over a much narrower, but generally higher range than our SGD estimates, from 3.4 to 5.2 $\times 10^6$ m^3 d^{-1}, however, this is considered an upper limit as we did not correct for aquifer withdrawals, loss via direct overland flow to the estuary through small creeks and streams, and inputs landward of the Franklin Lock (any of which could be substantial terms in this region). A more comprehensive water balance was beyond the scope of this study and is provided here merely for context.

Table 6
Estimates of groundwater discharge to the Caloosahatchee River Estuary.

(10^6 m^3/day)				
Method	Apr-09	Oct-09	Apr-10	Oct-10
Total SGD (Ra isotopes)[1]	0.37	0.20	0.08	1.28
Terrestrial SGD (Ra isotopes)[1]	0.16	0.19	0.08	1.26
SGD (water balance)[2]	5.19	3.36	4.55	5.11
Franklin Lock Discharge[3]	1.84	1.93	5.20	0.91

[1] Franklin Lock to Gulf of Mexico inlet.
[2] Does not account for anthropogenic withdrawals and includes input landward of the Franklin Lock.
[3] Mean daily flow for 2.5 weeks proceeding the field study.

4.4. Groundwater nutrient fluxes to the Caloosahatchee River Estuary

The central goal of this study is the application of the radium approach to determine groundwater nutrient fluxes. The impact of nutrient fluxes on the ecology of the Caloosahatchee River estuary has been relatively well documented (e.g. Brand and Compton, 2007; Lapointe and Bedford, 2007), though the potential role of sources other than freshwater releases at the Franklin Lock dam has not been fully evaluated. For SGD, the approach via the radium tracer is relatively simple in that the nutrient flux is the product of the Ra-derived SGD flux and the average nutrient concentration in the groundwater endmember:

$$F_N = F_{SGD} * N_{gw}$$

where F_N is the nutrient flux, F_{SGD} is the SGD water flux, and N_{gw} is the mean concentration of the nutrient in groundwater. However, it should be noted that, in most applications, such a calculation does not take into account the potential nutrient transformations that may occur in the subterranean estuary (Moore, 1999). These include such processes as denitrification, sorption of phosphorous to Fe (hydr)oxides, and desorption of ammonium during seawater intrusion (Charette and Sholkovitz, 2002). Our study therefore has focused on sampling wells located as close to the location of discharge as possible, i.e. at the estuarine land-water interface and not at inland wells.

We focused on three classes of macronutrients: total dissolved nitrogen (TDN, includes both organic and inorganic forms that pass through a 0.22 μm filter), dissolved inorganic nitrogen (DIN, includes nitrate, nitrite and ammonium), and soluble reactive phosphate (SRP, includes inorganic dissolved phosphate only). We sorted the groundwater nutrient data by groundwater source in the same manner as the groundwater Ra data. Except for DIN and samples from the April 2010 study, the average groundwater nutrient concentrations were similar for all time periods. The variability between the April 2010 data and other seasons could be due to the fact that we only sampled a subset of the wells from 2009 in 2010 and that in 2010 we had more piezometer samples than in 2009. For the terrestrial surficial aquifer groundwater samples, TDN averaged 64.1 ± 30.3 μM, while DIN and SRP averaged 34.9 ± 21.8 and 6.5 ± 9.4 μM, respectively. Note that DIN was ~50% of the TDN, therefore dissolved organic nitrogen is an important component of the total nitrogen in the aquifer. For the marine groundwater samples, TDN averaged 80.1 ± 60.0 μM, while DIN and SRP averaged 39.9 ± 38.2 and 3.9 ± 3.2 μM, respectively. While nitrate was detected in many of our samples (Tables 1–4), the dominant form of DIN was ammonium and we attribute this (along with the relatively high SRP concentrations) to reducing conditions within the aquifer. This dominance of ammonium is consistent with Kroeger et al. (2007), who reported on the nutrient biogeochemistry of shallow groundwater for the Tampa Bay watershed. In contrast, Kroeger et al. (2007) found 2–3 times higher TDN, DIN, and SRP in terrestrial groundwater from Tampa Bay aquifer but similar values for marine groundwater (salinity >2). Furthermore, our DON/TDN fraction was quite similar to the Kroeger et al. study (50–52% vs. 55% here). Also, the inorganic N:P ratio of the groundwater between our studies was similar 5.4–9.8 (this study) vs. 2.5–8.7, suggesting that (in the absence of additional N or P sources to the estuary), SGD-nutrient fueled primary productivity within the estuary would be N limited.

Since we could not discern a temporal trend in groundwater nutrients, we used average values that included data from all four sampling periods in our groundwater flux estimates; furthermore, we calculated the terrestrial and marine SGD fluxes independently reporting the sum total values in Table 7 and Fig. 11. With this approach, the groundwater-derived nutrient fluxes will generally scale with the SGD estimates from Table 6. For TDN, the groundwater flux to the estuary ranged from a lower limit of 76 kg d^{-1} (April 2010) to a maximum value of 1160 kg d^{-1} (April 2009) with an average of 450 ± 490 kg d^{-1} for the four time periods (Fig. 11a). For DIN, SGD fluxes ranged from 42 to 630 kg d^{-1} with an average of

Table 7
Nutrient loading estimates for the Caloosahatchee River estuary from submarine groundwater and Franklin Lock discharges.

	TDN		DIN		SRP	
	SGD	Franklin Lock	SGD	Franklin Lock	SGD	Franklin Lock
Time period	(kg/day)					
Apr-09	377	2057	194	295	58	140
Oct-09	179	2133	97	85	40	191
Apr-10	76	6219	42	2171	17	258
Oct-10	1159	869	630	237	258	16
Average	448	2819	241	697	93	151

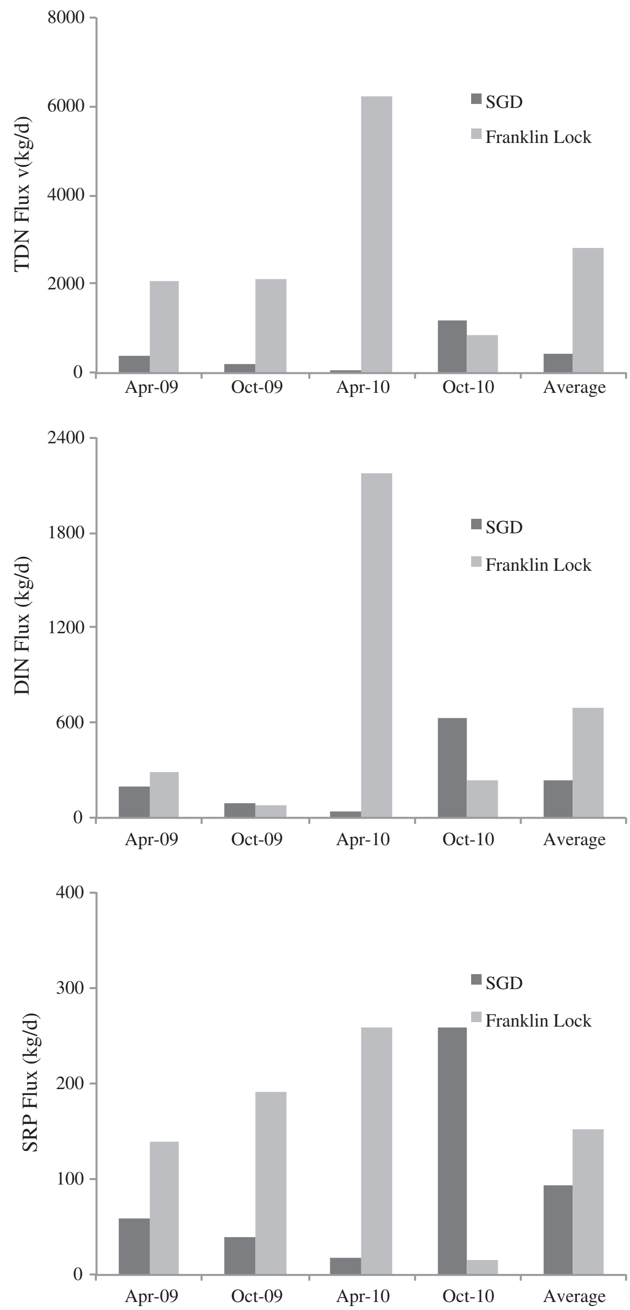

Fig. 11. Nutrient loading to the Caloosahatchee River estuary from submarine groundwater discharge and the Franklin Lock dam for the four sampling periods.

Please cite this article as: Charette, M.A., et al., Submarine groundwater discharge in a river-dominated Florida estuary, Mar. Chem. (2013), http://dx.doi.org/10.1016/j.marchem.2013.04.001

241 ± 267 kg d^{-1} (Fig. 11b). Lastly, SRP SGD fluxes were between 17 and 258 kg d^{-1} with an average of 93 ± 111 kg d^{-1} (Fig. 11c).

We compared these SGD nutrient fluxes with estimates of estuarine nutrient loading from freshwater releases through the Franklin Lock dam (Fig. 6a–c), which has been documented as a major source of nutrients to the Caloosahatchee River estuary (Brand and Compton, 2007). The inorganic N/P ratio of SGD during all periods was generally low (2.4–3.3), but similar to the N/P ratio of the river; both source terms N/P ratios suggest that N is the limiting nutrient for primary productivity within the estuary. The Franklin Lock fluxes were derived from the freshwater fluxes in Table 6 and the nutrient concentration (TDN, DIN, or SRP) for the station landward of the lock during a given sampling period (rather than study averages as was used to derive the SGD fluxes). On average, for TDN, the surface water freshwater fluxes exceed the SGD fluxes by a factor of ~6. However, the SGD fluxes of DIN and SRP, significantly more bioavailable nutrient species compared with TDN, were only 3 and 1.5 times lower than the river flux despite the river average being skewed high by the above average April 2010 freshwater releases through the lock. Excluding this time period, the SGD DIN and SRP fluxes were on average equal to or higher than the river flux by 50%. Hence, SGD-derived DIN fluxes may exert a significant control on Caloosahatchee River estuary productivity during dry periods.

5. Conclusions

Radium fluxes from the Caloosahatchee River estuary to the Gulf of Mexico were 10% of the Mississippi River flux despite much lower freshwater input. We attribute this to higher rates of SGD as well as an aquifer lithology that supports higher groundwater Ra activities via U enriched soils and sediments. Results from both radium and a hydrologic water balance are suggestive of a substantial input of groundwater to the Caloosahatchee River estuary. Groundwater is highly enriched in nitrogen and phosphate, making groundwater an important component of the local nutrient demand of bloom forming algae. The major form of nitrogen in groundwater is as inorganic nitrogen, specifically ammonium. This highly labile form of nitrogen is likely rapidly consumed within the estuary by primary producers (both macro- and microalgae). Lastly, groundwater fluxes are highly seasonal in nature, a function of precipitation over the watershed averaged on ~yearly timescales. During extended dry periods when water is not released from the Franklin Lock, groundwater will remain a substantial source of nutrients to the system.

Acknowledgments

This work greatly benefited from discussions with project partners Drs. Larry Brand, Ai Ning Loh, Eric Milbrandt, and Mike Parsons. Two anonymous reviewers provided comments that improved the manuscript considerably. Access to the monitoring wells was kindly provided by Scott Summerall of the Lee County (FL) Natural Resources Department. Leslie Haynes and Bob Wasno from Florida Gulf Coast University were the boat operators during our offshore and estuary surveys. Drs. Christopher Buzzelli and Peter Doering of the South Florida Water Management District, West Palm Beach, FL provided estimates of the volume and surface area of the estuary. Funding was provided to M.A.C. by the Cove Point Foundation, National Science Foundation (OCE-0751525), and the city of Sanibel/Lee County, Florida for the "Drift Algae Study".

References

Abtew, W., 2004. Evapotranspiration in the Everglades; Comparison of Bowen Ratio Measurements and Model Estimations. Water Quality Assessment Division, South Florida Water Management District, West Palm Beach, Florida (July).

Boehm, A., Paytan, A., Shellenbarger, G.G., Davis, K.A., 2006. Composition and flux of groundwater from a California beach aquifer: Implications for nutrient supply to the surf zone. Continental Shelf Research 26, 269–282.

Brand, L.E., Compton, A., 2007. Long-term increase in Karenia brevis abundance along the Southwest Florida Coast. Harmful Algae 6 (2), 232–252.

Burnett, W.C., et al., 2006. Quantifying submarine groundwater discharge in the coastal zone via multiple methods. Science of the Total Environment 367 (2–3), 498–543.

Charette, M.A., 2007. Hydrologic forcing of submarine groundwater discharge: Insight from a seasonal study of radium isotopes in a groundwater-dominated salt marsh estuary. Limnology and Oceanography 52 (1), 230–239.

Charette, M.A., Buesseler, K.O., 2004. Submarine groundwater discharge of nutrients and copper to an urban subestuary of Chesapeake bay (Elizabeth River). Limnol. Oceanogr. 49 (2), 376–385.

Charette, M.A., Sholkovitz, E.R., 2002. Oxidative precipitation of groundwater-derived ferrous iron in the subterranean estuary of a coastal bay. Geophys. Res. Lett. 29, 81–85.

Charette, M.A., Buesseler, K.O., Andrews, J.E., 2001. Utility of radium isotopes for evaluating the input and transport of groundwater-derived nitrogen to a Cape Cod estuary. Limnol. Oceanogr. 46 (2), 465–470.

Cowart, J.B., Burnett, W.C., 1994. The distribution of uranium and thorium decay-series radionuclides in the environment — a review. J. Environ. Qual. 23 (4), 651–662.

Crotwell, A.M., Moore, W.S., 2003. Nutrient and radium fluxes from submarine groundwater discharge to Port Royal Sound, South Carolina. Aquat. Geochem. 9 (3), 191–208.

Cunningham, K.J., Locker, S.D., Hine, A.C., Bukry, D., Barron, J.A., Guertin, L.A., 2001. Surface-geophysical characterization of groundwater systems of the Caloosahatchee River basin, southern Florida. 2001-4084. 2001–4084.

Gonneea, M.E., Morris, P.J., Dulaiova, H., Charette, M.A., 2008. New perspectives on radium behavior within a subterranean estuary. Marine Chemistry 109 (3–4), 250–267.

Hu, C.M., Muller-Karger, F.E., Swarzenski, P.W., 2006. Hurricanes, submarine groundwater discharge, and Florida's red tides. Geophys. Res. Lett. 33 (11).

Jiang, L., Islam, S., Guo, W., Jutla, A.S., Senarath, S.U.S., Ramsay, B.H., Eltahir, E.A.B., 2009. A satellite-based daily actual evapotranspiration estimation algorithm over South Florida. Glob. Planet. Change 67, 62–67.

Krest, J.M., Moore, W.S., Rama, 1999. Ra-226 and Ra-228 in the mixing zones of the Mississippi and Atchafalaya Rivers: indicators of groundwater input. Mar. Chem. 64 (3), 129–152.

Krest, J.M., Moore, W.S., Gardner, L.R., Morris, J.T., 2000. Marsh nutrient export supplied by groundwater discharge: evidence from radium measurements. Global Biogeochem. Cycles 14 (1), 167–176.

Kroeger, K.D., Swarzenski, P.W., Greenwood, W.J., Reich, C., 2007. Submarine groundwater discharge to Tampa Bay: nutrient fluxes and biogeochemistry of the coastal aquifer. Mar. Chem. 104 (1–2), 85–97.

Krulikas, R.K., Geise, G.L., 1995. Recharge to the surfical aquifer system in Lee and Hendry Counties, Florida. 95-4003.

Lapointe, B.E., Bedford, B.J., 2007. Drift rhodophyte blooms emerge in Lee County, Florida, USA: evidence of escalating coastal eutrophication. Harmful Algae 6 (3), 421–437.

Li, Y.-H., Chan, L.-H., 1979. Desorption of Ba and ^{226}Ra from river-borne sediments in the Hudson Estuary. Earth Planet. Sci. Lett. 43, 343–350.

Martin, J.B., Cable, J.E., Smith, C., Roy, M., Cherrier, J., 2007. Magnitudes of submarine groundwater discharge from marine and terrestrial sources: Indian River Lagoon, Florida. Water Resour. Res. 43 (5).

Michael, H.A., Mulligan, A.E., Harvey, C.F., 2005. Seasonal oscillations in water exchange between aquifers and the coastal ocean. Nature 436, 1145–1148.

Miller, R.L., Kraemer, T.F., McPherson, B.F., 1990. Radium and radon in Charlotte Harbor Estuary, Florida. Estuar. Coast. Shelf Sci. 31, 439–457.

Monsen, N.E., Cloern, J.E., Lucas, L.V., Monismith, S.G., 2002. A comment on the use of flushing time, residence time, and age as transport time scales. Limnol. Oceanogr. 47 (5), 1545–1553.

Moore, W.S., 1996. Large groundwater inputs to coastal waters revealed by Ra-226 enrichments. Nature 380 (6575), 612–614.

Moore, W.S., 1997. High fluxes of radium and barium from the mouth of the Ganges-Brahmaputra river during low river discharge suggest a large groundwater source. Earth Planet. Sci. Lett. 150 (1–2), 141–150.

Moore, W.S., 2000. Ages of continental shelf waters determined from ^{223}Ra and ^{224}Ra. J. Geophys. Res. 105 (C9), 22,117–23,894.

Moore, W.S., Reid, D.F., 1973. Extraction of radium from natural-waters using manganese-impregnated acrylic fibers. J. Geophys. Res. 78 (36), 8880–8886.

Moore, W.S., Arnold, R., 1996. Measurement of Ra-223 and Ra-224 in coastal waters using a delayed coincidence counter. Journal of Geophysical Research-Oceans 101 (C1), 1321–1329.

Moore, W.S., Blanton, J.O., Joye, S., 2006. Estimates of flushing times, submarine groundwater discharge, and nutrient fluxes to Okatee River, South Carolina. J. Geophys. Res. Oceans 111 C09006.

Paytan, A., Shellenbarger, G.G., Street, J.H., Gonneea, M.E., Davis, K., Young, M.B., Moore, W.S., 2006. Submarine groundwater discharge: an important source of new inorganic nitrogen to coral reef ecosystems. Limnol. Oceanogr. 51 (1), 343–348.

Qiu, C., Sun, D., 2009. Computation of Residence Time: Caloosahatchee Estuary. South Florida Water Management District.

Rama, Moore, W.S., 1996. Using the radium quartet for evaluating groundwater input and water exchange in salt marshes. Geochim. Cosmochim. Acta 60 (23), 4645–4652.

Reich, C., 2009. Investigation of Submarine Groundwater Discharge along the Tidal Reach of the Caloosahatchee River, Southwest Florida. Open-File Report 2009-1273, U.S. Geological Survey.

SFWMD, 2012. Caloosahatchee River Watershed Protection Plan Update. South Florida Water Management District.

Slomp, C.P., Van Cappellen, P., 2004. Nutrient inputs to the coastal ocean through submarine groundwater discharge: controls and potential impact. Journal of Hydrology 295 (1–4), 64–86.

Smith, C.G., Swarzenski, P.W., 2012. An investigation of submarine groundwater-borne nutrient fluxes to the west Florida shelf and recurrent harmful algal blooms. Limnol. Oceanogr. 57 (3), 471–485.

Swarzenski, P.W., Reich, C., Kroeger, K.D., Baskaran, M., 2007. Ra and Rn isotopes as natural tracers of submarine groundwater discharge in Tampa Bay, Florida. Mar. Chem. 104 (1–2), 69–84.

Veeh, H.H., Moore, W.S., Smith, S.V., 1995. The behavior of uranium and radium in an inverse estuary. Cont. Shelf Res. 15 (13), 1569–1583.

Weinstein, Y., et al., 2011. What Is the Role of Fresh Groundwater and Recirculated Seawater in Conveying Nutrients to the Coastal Ocean? Environmental Science & Technology 45 (12), 5195–5200.